Influence of facing vertical stiffness on reinforced soil wall design

Influence de la rigidité verticale du parement dans la conception des murs en sols renforcés

Damians I.P., Lloret A., Josa A.
Universitat Politècnica de Catalunya (UPC) – BarcelonaTech

Bathurst R.J.
Royal Military College of Canada

ABSTRACT: Current design practices for reinforced soil walls typically ignore the influence of facing type and foundation compressibility on the magnitude and distribution of reinforcement loads in steel reinforced soil walls under operational conditions. In this paper, the effect of the facing vertical stiffness (due to elastomeric bearing pads placed in the horizontal joints between panels) on load capacity of steel reinforced soil walls is examined in a systematic manner using a numerical modelling approach. Numerical modelling was carried out using the commercial finite element program PLAXIS. The numerical model was verified against measurements recorded for an instrumented 6 m-high wall reinforced with steel strips. The influence of the facing stiffness and backfill-foundation stiffness combinations on the vertical load through the facing and on the magnitude and distribution of the reinforcement loads was examined. For walls subjected to operational (working stress) conditions at end of construction, the numerical results confirm that the vertical stiffness of the facing and soil-stiffness combinations can have a great effect on the vertical facing loads and on the magnitude and distribution of the load mobilized in the soil reinforcement layers.

RÉSUMÉ: Les pratiques actuelles de conception des murs en sol renforcé ignorent généralement l'influence du type du parement et de la rigidité de la fondation sur l'ampleur et la répartition des charges de renforcement. Dans cet article, on utilise une approche par modélisation numérique pour examiner systématiquement l'effet de la rigidité du parement vertical (due à la présence de cales en élastomère placées dans les joints horizontaux entre panneaux) sur la capacité de charge des murs renforcés sol/acier. La modélisation numérique a été réalisée à l'aide du code commercial Éléments Finis PLAXIS. Le modèle numérique a été validé sur des mesures enregistrées lors de l'expérimentation d'un mur d'une hauteur de 6 m et renforcé par des bandes d'acier. Le modèle permet de tester l'influence de différentes combinaisons entre la rigidité du parement et celle du remblai-fondation sur les valeurs des charges verticales dans le parement et les efforts dans les éléments de renforcement. Pour les murs travaillant en conditions opérationnelles (sous efforts de service) à la fin de leur construction, les résultats numériques confirment que ces combinaisons ont un grand effet sur les charges verticales et la distribution des efforts mobilisés dans les couches de renforcement.

KEYWORDS: reinforced soil retaining walls, steel strips, facing panels, finite element modelling.

1 INTRODUCTION AND GENERAL APPROACH

The mechanical behaviour of reinforced soil walls is complicated due to the mechanical complexity of the component materials (including soil type/arrangement), their interactions, wall geometry, and the influence of method of construction. Most reinforced soil walls are designed assuming that the wall foundation is rigid and/or does not influence the magnitude and distribution of reinforcement loads under operational conditions. This assumption may not apply to walls constructed over compressible foundations. This paper describes the results of a series of numerical simulations that were carried out on a 6-m high wall with precast concrete panels with metallically reinforced soil and constructed with backfill (reinforced soil and retained fill) and foundation soils having different stiffness, and different number of horizontal joints (i.e. different height of the panel units) along the facing elevation.

The program PLAXIS (PLAXIS 2008) was used to carry out the numerical simulations. The reference case for model calibration is the instrumented 6 m-high precast panel facing wall reinforced with steel strips reported by Chida and Nakagaki (1979). All the results in the present study correspond to operational (working stress) conditions at the end of the construction.

2 NUMERICAL MODEL

2.1 *General*

The PLAXIS global geometry, structural components, and the numerical mesh to simulate the performance of the reference instrumented case are illustrated in Figure 1.

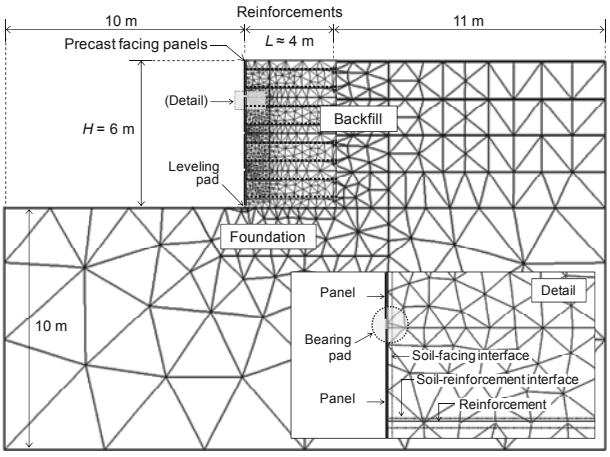

Figure 1. PLAXIS numerical model

2.2 *Materials properties*

2.3.1 *Soil*

Material properties for the soil zones (backfill and foundation) are summarized in Table 1. Two different stiffness of the backfill were considered to represent different scenarios due to the effects of compaction. The more compressible soil case (with assumed $E_{backfill}$ = 10 MPa) does not imply that poorly compacted soils should be used in the construction of these types of structures, but was used to ensure detectable differences between simulation outcomes. Moreover, the first meter of reinforced soil in contact with the facing is commonly constructed with less compaction energy and hence was assumed to have one half the stiffness of the fully compacted soil. Two other cases were assumed for the foundation soil; nevertheless, the actual foundation stiffness for the reference wall case was not reported by Chida and Nakagaki. The stiffness combinations in Table 1 result in four boundary cases to be examined.

Plane-strain boundary conditions were considered for the selection of the internal friction angle of the soils. The soil material properties also define the strength and stiffness of the interfaces between the soil and the structural elements (panels and reinforcement) using a reduction factor (R_i), which is the ratio of interface shear strength to shear strength of the surrounding soil. The values chosen for this factor in each case (soil-facing and soil-reinforcement) are based on reported data and actual mechanical behavior of these interactions.

Table 1. Model properties of the soil materials

Parameters	Foundation	Backfill	
		> 1.0 m from face	< 1.0 m from face
Unit weight (kN/m^3)	20	18	18
Cohesion (kPa)	1	1	1
Friction angle (º)	36	44	44
Dilatancy angle (º)	6	14	14
Elastic modulus (MPa)	10 – 1000	10 & 100	5 & 50
Poisson's ratio	0.3	0.3	0.3
Interface reduction factor	1	1	0.3 & 0.6

2.3.2 *Reinforcement*

Reinforcement elements were modelled using the "geogrid" PLAXIS elements as continuous sheets that have only axial stiffness and can transmit load to the surrounding soil through interface shear (R_i parameter). The equivalent linear-elastic axial stiffness of the geogrid element for each layer of reinforcement elements is computed as follows:

$$(EA)_{geogrid} = E_{reinforcement} A_{reinforcement} \frac{n_{reinforcements}}{L_{panel}} \quad (1)$$

Where: $E_{reinforcement}$ is the stiffness modulus of the reinforcement layers (200 GPa for steel); A_{strip} is the cross-sectional area of one strip (100 × 2.3 mm); n_{strips} is the number of strips along one panel (two strip-units), and L_{panel} is the panel width assumed as 1.5 m. The resulting axial stiffness of the geogrid element is about 60 MPa/m. Other analyses considering different axial stiffness modulus equivalent to other steel reinforced types (e.g. bar mats with axial stiffness about 40 MPa/m) do not generate significant variations from the results presented in this study.

2.3.3 *Facing-beam elements*

The facing was defined by PLAXIS "beam" elements, and is comprised of the panels and the elastomeric bearing pads. The bearing pads are installed in the horizontal joints between contiguous vertical panels and are used in practice to prevent concrete-to-concrete panel contact.

Material properties for the concrete facing panels and horizontal joints are summarized in Table 2. The material type, dimensions and number of bearing pads can vary between projects (Neely and Tan 2010). The same Equation 1 can be used to obtain the parametrical values of the bearing pad elements (Damians et al 2013). In the present analyses, two EPDM (ethylene propylene diene monomer (M-class) rubber) bearing pads were assumed in each horizontal joint between per panel width.

Table 2. Model properties of the beam elements

Parameters	Panels	Bearing pads (EPDM)
Axial stiffness (MN/m)	6.0	0.1
Bending stiffness (kN/m^2/m)	11	0.3
Weight (kN/m/m)	4.5	0.2
Poisson's ratio	0.15	0.49

3 RESULTS

3.1 *Numerical and reported physical data comparison*

Numerical predicted vertical loads at the base of the facing panels and the reinforcement loads were compared to values reported by Chida and Nakagaki (1979) during calibration of the numerical model.

3.1.1 *Vertical loads under facing*

Damians et al. (2013) have shown from a review of instrumented case studies that the vertical load at the base of a precast facing wall with steel reinforced soil elements is greater than the self-weight of the panels. The vertical load under facing is a combination of facing self-weight, soil-panel shear and reinforcement down-drag loads, which generate reported load factors from 1.8 to 4.7 times the self-weight of the panels in steel reinforced soil walls (a value of 2.1 is computed for the reference wall reported by Chida and Nakagaki). It should be noted that the studied cases are restricted to steel reinforced soil walls. However, there are similar data for an instrumented full-scale 6-m high geosynthetic-reinforced soil wall with incremental concrete panels constructed in the laboratory (Tariji et al. 1996); the computed vertical load factor is 2.2 for this structure.

Figures 2a and 2b summarize results that take into account the effect of the backfill and foundation stiffness scenarios and the backfill-facing interface shear strength (R_i value of 0.3 and 0.6).

The data show that the larger R_i-value assumed results in a range of total vertical facing loads that vary from the reported value of 53.3 kN/m for the reference case. Assuming a value of R_i = 0.3 generates four stiffness scenarios that include the measured case study value more accurately (modifying the $E_{backfill}$ from 100 to 10 MPa when $E_{foundation}$ is 1000 MPa, or modifying $E_{foundation}$ from 1000 to 10 MPa when $E_{backfill}$ is constant at 100 MPa).

Typically, the recommended interface shear strength factor values are about 0.6 times the shear strength of the surrounding soil. However, analysis of a wall reported by Runser et al. (2001) showed that a value of R_i = 0.3 was gave more accurate

predictions (Damians et al. 2013). This value was adopted in the current study.

3.1.2 *Reinforcement loads*

In Figure 3 are shown the results of the reinforcement tensile loads obtained from numerical modelling and comparison with measured data for selected strips at different elevations. The reinforcement length considered in this study is 0.6 – 0.7 times the total wall height. Steel strips with lengths from 4.0 to 5.0 m were used in the reference case study, so all locations along any reinforcement layer are normalized with the respect to the layer length.

The presented results show good agreement between the numerical model results and measured data. The backfill-foundation stiffness combination results give different tensile-load distributions in the reinforcement layers. The effect of the less-compacted soil near the facing can be clearly detected with the discontinuity at a normalized distance from 0 to 0.25.

a) $R_i = 0.3$

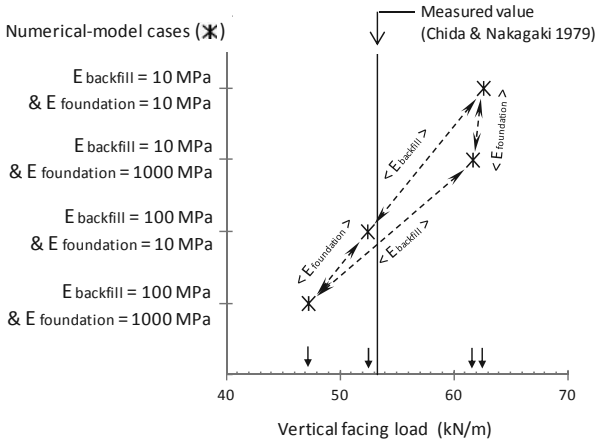

b) $R_i = 0.6$

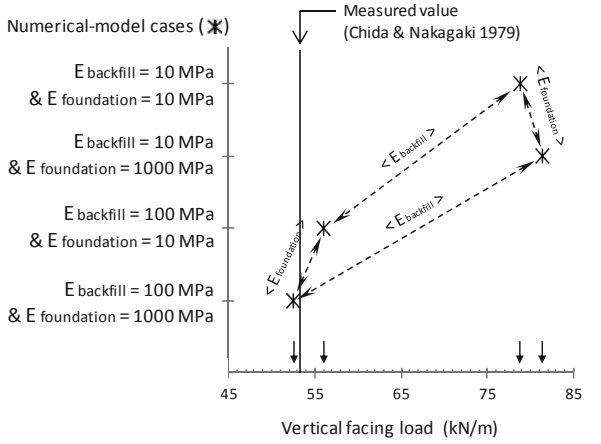

Figure 2. Total vertical loads under the facing assuming soil-facing interface reduction factor $R_i = 0.3$ (a), and $R_i = 0.6$ (b)

3.2 *Influence of vertical facing stiffness*

As noted earlier, the vertical facing stiffness was modified by changing the number of horizontal joints along the facing height of the wall. The reported case (base-case) had three horizontal joins (four panels of 1.5 m-height). Three other cases were considered to investigate the effect of the vertical facing stiffness (see Figure 4).

Figure 5 shows the numerical model reinforcement tensile-loads with respect to the number of horizontal joints. The values correspond to the maximum load ($T_{maximum}$) of all the reinforcement strips, its related strip, and the normalized distance of T_{max} to the facing in the strip. Reported values obtained from Chida and Nakagaki (1979) are also shown.

First, it can be noted that there is little difference in the predicted T_{max} value with respect to the backfill and foundation stiffness combinations (less than 4 kN/m in the case with more divergence, i.e. $E_{backfill}$ = 100 MPa and $E_{foundation}$ =10 MPa combination). All the T_{max} values (numerical and measured) are located at the bottom zone of the wall (all at the layer located at 1.13 m, except the numerical case with $E_{backfill}$ = 100 MPa and $E_{foundation}$ =10 MPa). With respect to their location in the reinforcement (normalized distance from the facing), all the T_{max} values are located between 0.3 and 0.5.

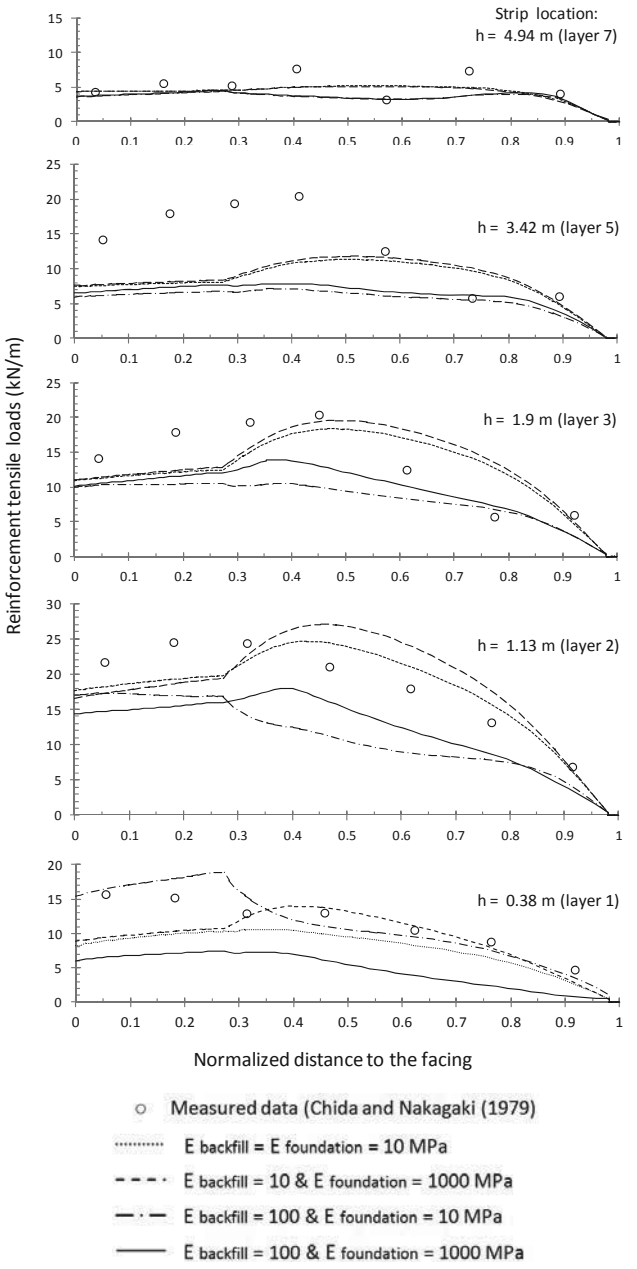

Figure 3. Tensile-load distribution of the wall reinforcements at the end of construction. (Normalized distance = distance to the facing of a stress i-point / total length of the reinforcement)

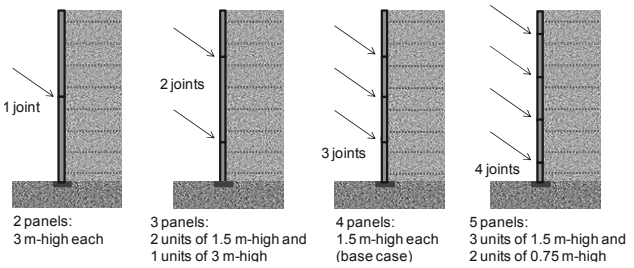

Figure 4. Schema about the horizontal joint options considered

Figure 6 shows the effect of the foundation stiffness and the vertical facing stiffness on the total vertical loads at base of the facing. Three additional foundation stiffness cases are considered here in order to obtain more data points. It can be observed that higher values of the foundation stiffness (elastic modulus) generate lower values of the total vertical load under the facing. If the total vertical load under the facing with respect to the number horizontal joints is analyzed (Figure 6), a significant influence of the vertical facing stiffness on the results can be noted. This influence is less relevant if the lowest modulus of the backfill soil is assumed (i.e. $E_{backfill}$ = 10 MPa, which generates a range of about 3 kN/m between boundary cases). If the backfill soil is assumed with higher stiffness value ($E_{backfill}$ = 100 MPa), the variation of the vertical load is more significant with a range of 15 kN/m for the single joint case, and 20 kN/m for the four joint case.

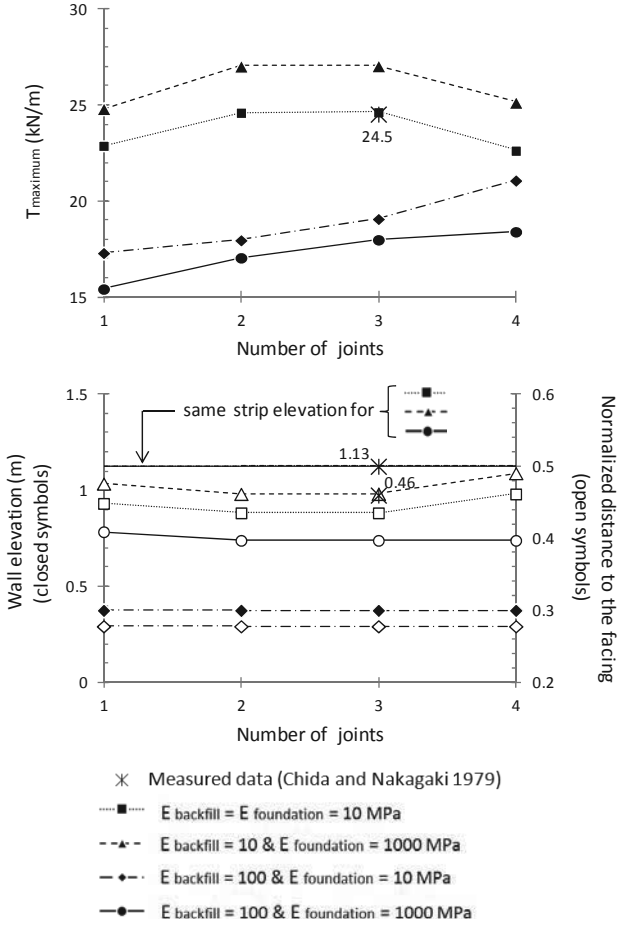

Figure 5. Maximum reinforcement loads (T_{max}) with respect to the number of horizontal joints and backfill-foundation stiffness combination (upper figure), and the T_{max} location in the backfill (reinforcement layer and distance to the facing; bottom figure)

4 CONCLUSIONS

The mechanical behaviour of reinforced soil walls is complicated due to the mechanical complexity of the component materials, their interactions, wall geometry and soil type/arrangement, in addition to the unquantifiable effects of construction method and quality. Nevertheless, current design methods are typically based on classical notions of soil and reinforcement ultimate strength. Furthermore, internal stability design using conventional analytical solutions assumes that the compressibility of the foundation soil does not influence reinforcement loads.

The numerical simulation results in the current study demonstrate, first, that vertical loads at the base of the facing are affected directly by the backfill and foundation stiffness scenario and the soil-facing interface shear strength; second, there is a significant variation of reinforcement tensile load results depending on the combination of the backfill and foundation stiffness values; and third, the vertical stiffness of the facing (represented by the number of horizontal joints along the facing, that can be also be understood as different thicknesses of the bearing pad elements) produce significantly different effects on the vertical facing load and the reinforcement tensile loads. These three outcomes cannot be predicted for walls under operational (working stress) conditions using current strength-based design methods for the calculation of reinforcement loads.

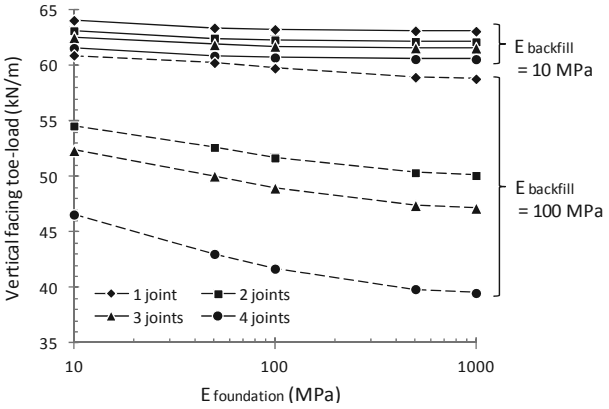

Figure 6. Vertical facing toe-load comparison with facing, foundation and backfill stiffness

5 REFERENCES

Chida, S. and Nakagaki, M. 1979. Test and experiment on a full-scale model of reinforced earth wall. *Proceedings of the International Conference on Soil Reinforcement*, Paris, France, Vol. 2, pp. 533-538.

Damians, I.P., Bathurst, R.J., Josa, A., Lloret, A. and Albuquerque, P.J.R. 2013. Vertical facing loads in steel reinforced soil walls. *ASCE Journal of Geotechnical & Geoenvironmental Engineering* (in press).

Neely, W.J. and Tan, S.L. 2010. Effects of second order design factors on the behaviour of MSE walls. Earth Retention Conference 3. Earth Retaining Structures Committee of the Geo-Institute of ASCE. Geotechnical Special Publications (GSP) n. 208. *Proceedings of the 2010 Earth Retention Conference*, Bellevue, Washington, August 1-4, 2010, pp. 522-530.

PLAXIS. 2008. Reference Manual, 2D - Version 9.0. PLAXIS B.V., Delft University of Technology, The Netherlands.

Runser, D.J., Fox, P.J. and Bourdeau, P.L. 2001. Field performance of a 17 m-high reinforced soil retaining wall. *Geosynthetics International*, 8(5): 367-391.

Tajiri, N., Sasaki, H., Nishimura, J., Ochiai, Y. and Dobashi, K. 1996. Full-scale failure experiments of geotextile-reinforced soil walls with different facings. *IS-Kyushu 96, 3rd International Symposium on Earth Reinforcement*, Fukuoka, Japan, pp. 525-530.